Journal of Analytical and Applied Pyrolysis 122 (2016) 175–182

Contents lists available at ScienceDirect

Journal of Analytical and Applied Pyrolysis

journal homepage: www.elsevier.com/locate/jaap

Isoconversional thermal and pyrolytic GC–MS analysis of street samples of hashish

Mohammad S. Iqbal[a,*], Muhammad U.A. Khan[b], Jamshed Akbar[c], Muhammad A. Shad[b], Rashid Masih[a], Muhammad T. Chaudhary[d]

[a] Department of Chemistry, Forman Christian College, Lahore 54600, Pakistan
[b] Department of Biochemistry, Bahauddin Zakariya University, Multan 60000, Pakistan
[c] Department of Chemistry, University of Sargodha, Sargodha 40100, Pakistan
[d] Forensic Toxicology Unit, Punjab Forensic Science Agency, Home Department, Government of the Punjab, Thokar Niaz Baig, Multan Road, Lahore, Pakistan

ARTICLE INFO

Article history:
Received 13 March 2016
Received in revised form
30 September 2016
Accepted 30 September 2016
Available online 11 October 2016

Keywords:
Cannabis
Hashish
Narcotics
Isoconversional analysis
Thermal degradation
Pyrolysis GC–MS

ABSTRACT

Thermal decomposition of hashish, a widely used illicit drug, was studied by isoconversional and pyrolytic GC–MS analysis. An accurate value of activation energy was determined by the B-1.92 method, which was used to determine degradation mechanism, impact of destruction by incineration of the drug on environment. The thermograms exhibited a weight loss of 11–19% from ambient to 463 K due to moisture content. Major degradation occurred in the range 463–643 K. The average activation energy was found to be ~121 kJ mol^{-1} that suggested rapid volatilization of the material in the temperature range. The variation of activation energy with conversion suggested a multistep degradation of the samples. The mechanism of degradation was found to be a second order decomposition representing an exothermic chemical change. The residue at 1073 K was analyzed by SEM-EDS and found to contain C, O, P, S, K, Mg, Ca, Al and Si to various extents; C and O were present in substantial amounts. Pyrolytic GC–MS analysis identified cannabidiol, limonene, β-caryophyllene and pyrolytic products of acetaminophen and dehydrophenacetin as the major decomposition products. This study shows that the incineration process does not completely destroy the drug, rather it throws large quantities of drug-related toxic substances into the environment. The pyrolysis GC–MS showed that the characteristic peak due to cannabidiol can be used as a signature of the drug in biological samples.

1. Introduction

Street samples of hashish, commonly known as "hash", mainly contain cannabinoids mixed with other drugs and adulterants. The preparations are compressed and/or purified stalked resin glands (trichomes) collected from unfertilized buds of cannabis plant. The active ingredients are Δ^9-tetrahydrocannabinol (Δ^9-THC) and other cannabinoids [1]. The use of hashish as a medicine and recreational drug dates back to 3rd millennium BC [2]. Although it is currently illegal to use or consume hashish in any form everywhere in the world, but its use is increasing day by day. Large quantities are being seized every year around the world. The seized samples are generally being destroyed by incineration. We think that incineration is not a suitable process for destruction as it may adversely affect our environment and the personnel involved. The information on the environmental impact of destruction by incineration is very rare in literature as only a few studies on thermal analysis have been reported [3]. Therefore, one of the object of this study was to carry out complete thermal analysis combined with GC–MS.

Thermal analysis techniques including thermogravimetric analysis (TGA) and differential scanning calorimetry (DSC) are extremely helpful in characterizing materials by determining kinetic parameters including thermal stability, activation energy (E_a) and degradation mechanism. A number of model-free isoconversional methods have been reported for determination of E_a from TGA and DSC data. Recently, accuracy of these methods has been investigated and they have been classified as Type A methods, which make no mathematical approximations (e.g. Friedman methods), and Type B methods, which make use of various approximations to solve the temperature integral (e.g. Kissinger-Akahira-Sunose or KAS method) [4]. This rigorous study has identified that the most popular Ozawa method is highly inaccurate, whereas the KSA method has about 1% inaccuracy. The

* Corresponding author.
E-mail address: saeediq50@hotmail.com (M.S. Iqbal).

http://dx.doi.org/10.1016/j.jaap.2016.09.026
0165-2370/

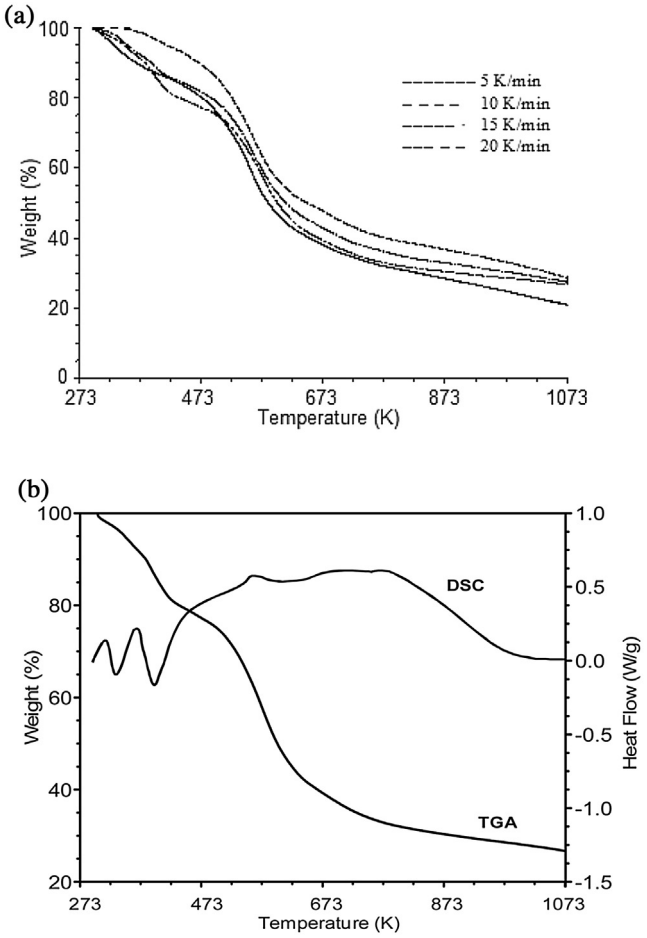

Fig. 1. TGA (a) and DSC (b) curves for hashish.

author was able to demonstrate that highly accurate E_a can be determined by use of the optimized equation (Eq. (1)):

$$\ln\left[\frac{\beta}{T^{1.92}}\right] = -1.0008\frac{E_a}{RT} + \text{Constant}. \quad (1)$$

where β is the heating rate; R the general gas constant; E_a and T are the activation energy and temperature at α, the degree of conversion i.e. $(w_o - w_t)/(w_o - w_f)$, where w_t is the weight of the sample at any temperature $T(K)$, w_o the initial weight and w_f the final weight at the temperature where the mass loss is almost negligible. In the present work we have made use of this equation for determination of E_a.

The thermal degradation products can be identified by GC–MS analysis after pyrolysis [5,6]. Pyrolysis GC–MS is a powerful technique to determine the signatures of drug molecules in a variety of samples.

2. Experimental

2.1. Materials

Six hashish samples were collected directly from the addicts in different areas of Lahore city. They were preserved in zip-lock polyethylene bags and stored under refrigeration till analysis. The solvents used were acetone, methanol, *n*-hexane, carbon tetrachloride and chloroform from E. Merck, Germany and were used without further purification.

2.2. Thermogravimetry and differential scanning calorimetry

The samples (2.5–7.0 mg) were analyzed by a simultaneous thermal analyzer SDT, Q-600 (TA instruments, USA) at 5, 10, 15 and 20 K min^{-1} heating rates from ambient (about 298 K) to 1073 K under nitrogen atmosphere (@ 100 cm^3 min^{-1}). TGA and DSC scans were obtained, and data were analyzed by use of Universal Analysis 2000 software, version 4.2E (TA Instruments, USA) and MS Excel® 2007.

2.3. Degradation kinetics

Thermal degradation kinetics of the samples was investigated by isoconversional (model-independent) method using the recently reported Type B-1.92 Eq. (1) affording a highly accurate E_a value [4]. In the B-1.92 method, straight-line plots of $\log(\beta/T^{1.92})$ vs $1/T$ were obtained. From the slopes of these plots, E_a values were determined.

The degradation mechanism, $g(\alpha)$, was determined by use of master-plot method, Eq. (2) [7].

$$\frac{g(\alpha)}{g(0.5)} = \frac{p(x)}{p(x_{0.5})} \quad (2)$$

where $x = E_a/RT$; $p(x) = \int_x^\infty \frac{\exp(-x)}{x^2}dx$; $g(0.5)$ and $p(x_{0.5})$ are theoretical and experimental reaction models at $\alpha = 0.5$, respectively. The theoretical master plots were constructed by plotting $g(\alpha)/g(0.5)$ against α for various $g(\alpha)$ functions (Table 1) [8]. The experimental master plots were constructed by plotting $p(x)/p(x_{0.5})$ against α. The $p(x)$ integral was solved by the method reported by Starink (Eq. (3)) [4].

$$p(x) = \frac{e^{(-1.0008x - 0.312)}}{x^{1.92}} \quad (3)$$

The pre-exponential factor, A, was calculated by use of compensation effect relationship [9] according to Eq. (4).

$$\ln A = a + bE_a \quad (4)$$

where a and b are the compensation parameters, which were determined by model-fitting approach using Coats-Redfern Eq. (5).

$$In\frac{g(\alpha)}{T^2} = In\left[\left(\frac{AR}{\beta E_a}\right)\left(1 - \frac{2R\bar{T}}{E_a}\right)\right] - \frac{E_a}{TR} \quad (5)$$

where $\bar{T}$ is the average experimental temperature. The $g(\alpha)$ models used for solving Eq. (5) in the present work are listed in Table 1. By use of this equation plots of $\ln(g(\alpha)/T^2)$ vs $1/T$ yield a set of kinetic parameters, A and E_a. The parameters a and b were determined from the slope and intercept, respectively, from the plot between A and E_a values obtained from Eq. (5). The ln$A$ value was determined by substituting a, b, and average E_a from B-1.92 method in Eq. (4).

Isothermal plots at different temperatures were plotted by using the data obtained from isoconversional analysis. The time at a given conversion was determined by Eq. (6) [9].

$$t_\alpha = \frac{\int_0^{T_\alpha} \exp\left(-\frac{E_\alpha}{RT}\right)dT}{\beta \exp\left(-\frac{E_\alpha}{RT_0}\right)} \quad (6)$$

2.4. Residue analysis

The residue at 800 °C was analyzed by scanning electron microscopy (SEM) along with energy dispersive X-ray analysis by using Hitachi VP-SEM S-3400N equipped with energy dispersive X-ray spectrometric (EDS) facility (EMAX-Horiba). The elemental analysis in different regions of the residue was carried out.

Table 1
Various g(α) models used to describe solid-state kinetics.

No.	Code	Description	Model	Mechanism
Chemical process mechanisms				
1.	$F_{1/3}$	One-third order	$1-(1-\alpha)^{2/3}$	Chemical reaction
2.	$F_{3/4}$	Three-quarter order	$1-(1-\alpha)^{1/4}$	Chemical reaction
3.	$F_{3/2}$	One and a half order	$(1-\alpha)^{-1/2}-1$	Chemical reaction
4.	F_2	Second order	$(1-\alpha)^{-1}-1$	Chemical reaction
5.	F_3	Third order	$(1-\alpha)^{-2}-1$	Chemical reaction
Acceleratory rate equations				
6.	$P_{3/2}$	Mampel power law	$\alpha^{3/2}$	Nucleation
7.	$P_{1/2}$	Mampel power law	$\alpha^{1/2}$	Nucleation
8.	$P_{1/3}$	Mampel power law	$\alpha^{1/3}$	Nucleation
9.	$P_{1/4}$	Mampel power law	$\alpha^{1/4}$	Nucleation
Sigmoidal rate equations/Random nucleation and subsequent growth				
10.	A_1, F_1	Avrami-Erofeev equation	$-\ln(1-\alpha)$	Assumed random nucleation and its growth. $n=1$
11.	$A_{3/2}$	Avrami-Erofeev equation	$[-\ln(1-\alpha)]^{2/3}$	Assumed random nucleation and its growth. $n=1.5$
12.	A_2	Avrami-Erofeev equation	$[-\ln(1-\alpha)]^{1/2}$	Assumed random nucleation and its growth. $n=2$
13.	A_3	Avrami-Erofeev equation	$[-\ln(1-\alpha)]^{1/3}$	Assumed random nucleation and its growth. $n=3$
14.	A_4	Avrami-Erofeev equation	$[-\ln(1-\alpha)]^{1/4}$	Assumed random nucleation and its growth. $n=4$
15.	A_u	Prout-Tomkins equation	$\ln[\alpha/(1-\alpha)]$	Branching nuclei
Decceleratory rate equations/Phase boundary equations				
16.	R_1, F_0, P_1	Power law	α	Contracting disk
17.	R_2, $F_{1/2}$	Power law	$1-(1-\alpha)^{1/2}$	Contracting cylinder
18.	R_3, $F_{2/3}$	Power law	$1-(1-\alpha)^{1/3}$	Contracting sphere
Diffusion mechanism equations				
19.	D_1	Parabola equation	α^2	One-dimensional diffusion
20.	D_2	Valensi equation	$\alpha+(1-\alpha)\ln(1-\alpha)$	Two-dimensional diffusion
21.	D_3	Jander equation	$[1-(1-\alpha)^{1/3}]^2$	Three-dimensional diffusion, spherical symmetry
22.	D_4	Ginstling-Brounstein equation	$1-2\alpha/3-(1-\alpha)^{2/3}$	Three-dimensional diffusion, cylindrical symmetry
23.	D_5	Zhuravlev, Lesokin, Tempelman equation	$[(1-\alpha)^{-1/3}-1]^2$	Three-dimensional diffusion
24.	D_6	Anti-Jander equation	$[(1+\alpha)^{1/3}-1]^2$	Three-dimensional diffusion
25.		Anti-Ginstling-Brounstein equation	$1+2\alpha/3-(1+\alpha)^{2/3}$	Three-dimensional diffusion
26.		Anti-Jander equation	$[(1+\alpha)^{-1/3}-1]^2$	Three-dimensional diffusion

2.5. Pyrolytic GC–MS analysis

After identifying the decomposition stage through TGA, the pyrolytic products of the samples were collected at 423–673 K (@ 20 K min^{-1} with 5 min hold time at 673 K) in *n*-hexane, acetone, methanol, carbon tetrachloride and chloroform (10 cm^3 each) separately by use of an air-tight assembly after heating the samples (2.8–8.0 mg) in the thermal analyzer. The solutions thus obtained were subjected to GC–MS analysis by using 1 μL injection in splitless mode. The GC–MS system (Agilent Technologies, USA) consisted of: GC7890A gas chromatograph; MS5975C mass spectrometer with Triple-Axis detector; HP-5MS column (30m × 0.25 mm × 0.25 μm). The chromatographic and mass spectrometric conditions were: GC–Helium as carrier; flow rate 1.2 cm^3 min^{-1}; injector temperature 230 °C; column temperature 60 °C for 0 min then 10 °Cmin^{-1} to 300 °C for 5 min; ion source temperature 230 °C; MSD transfer line 280 °C; relative voltage 47 eV; mass range 50–600. Data were acquired and processed with the GC/MSD ChemStation. Compound identification was achieved by comparing the retention times with the standards and by use of relevant literature [10–13] and mass spectral library (NIST 05) of the GC–MS data system.

2.5.1. Method development for human tissue analysis

Blank samples of human lungs tissue obtained from a hospital and frozen in liquid nitrogen. The samples were stored at −60 °C until analysis. The sample (10–30 mg) was transferred to a 12 mm × 75 mm glass tube. To this 50 μL of Δ^9-THC solution (1.0 mg mL^{-1} ±5% in methanol, analytical standard for drug analysis from Sigma-Aldrich) was added and homogenized for 30 s and subjected to pyrolysis GC–MS analysis as described above. Percent recovery, precision, limit of detection and limit of quantitation were determined. The experiment was performed in triplicate.

Three real life samples of human lungs tissue (10–30 mg), obtained after post-mortem of addicts in a public hospital, were pyrolyzed and the products were analyzed by GC–MS after collection in *n*-hexane. All the procedures with human tissue were approved by the ethical committee of the Bahauddin Zakariya University.

3. Results and discussion

The hashish samples were resinous materials dark brown in color. Six samples from different parts of Lahore city were analyzed to study the variations if any. The results are discussed as follows.

3.1. Thermogravimetric analysis

The weight loss started occurring in the very beginning (Fig. 1a) due to presence of water and continued upto 463 K (stage I). At ambient to 423 K, the weight loss was about 22% which was confirmed to be due to water by as verified Karl-Fisher titration. Major decomposition (about 40%) occurred in the range 463–643 K (stage II) which was due to breakdown of the resinous material into different products as identified by pyrolytic GC–MS analysis (Section 3.2). Beyond 643 K a gradual weight loss occurred resulting in a residue of about 20%. The residue was subjected to further analysis by SEM-EDS. All the degradations were found to be exothermic (Fig. 1b) in nature. The E_a values of the stage II, calculated by B-1.92 method (Fig. 2a and b), changed gradually and produced a symmetric trend over all α values (Fig. 2c). The E_a values increased upto α = 0.55 and decreased thereafter. On this basis it can be suggested that it is a multistep degradation process involving various products, which was verified by GC–MS analysis of the pyrolytic products (Table 2).

The master plots constructed from the experimental data (Fig. 2d) appear to correlate best (R^2 = 0.996) representing the sec-

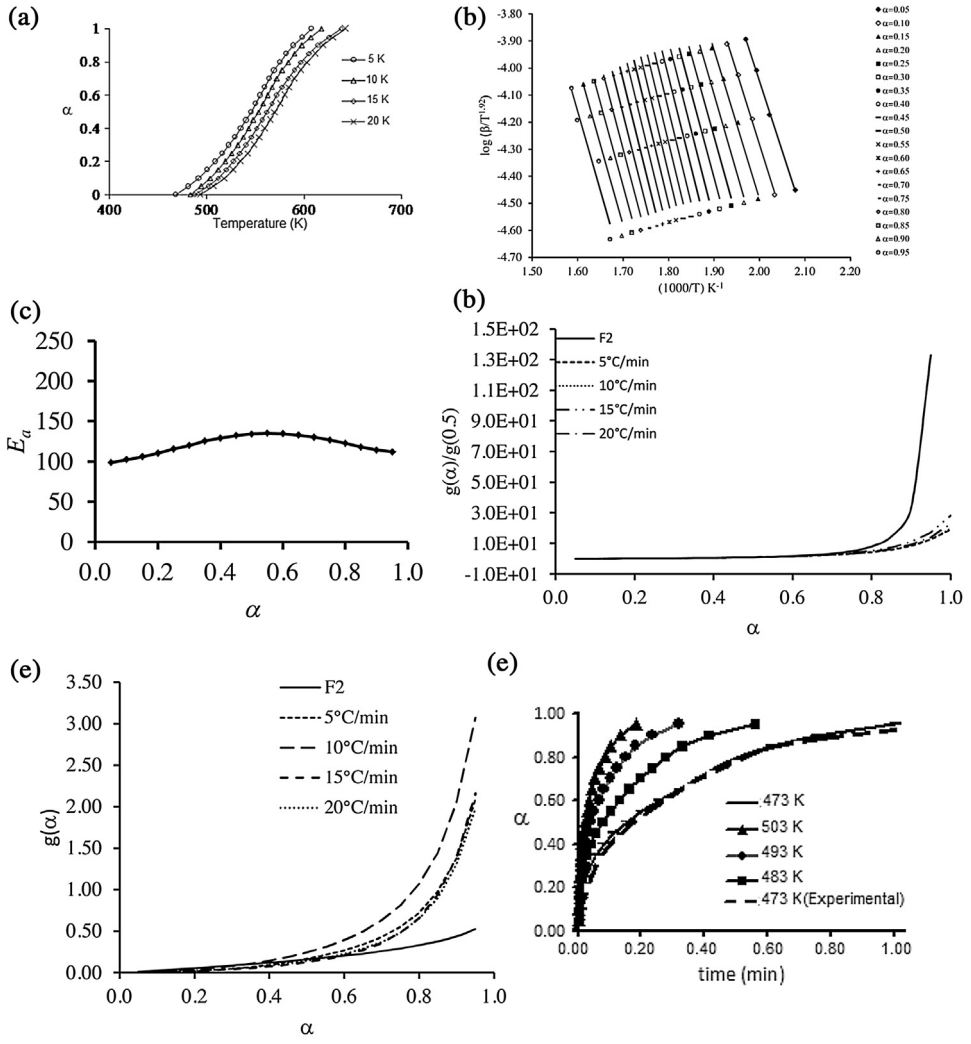

Fig. 2. Plots used for determination of thermal parameters: (a) α-T curve, (b) log ($\beta/T^{1.92}$) vs 1000/T plots for calculation of E_a, (c) Variation of E_a with degree of decomposition (α) of hashish, (d) Master plots for determination of kinetic model for decomposition of hashish, (e) Reconstructed g(α) plots from calculated kinetic parameters and (f) Isothermal time-α plots at different temperatures.

Table 2
Pyrolytic GC–MS data.

Compound	R.T. (min)	Mol. Mass	Mass fragments
Cannabidiol	20.463	314	314, 295, 258, 246, 231, 193, 174, 147, 121, 91, 67
α-Caryophyllene.	10.361	204	204, 189, 175, 161, 147, 133, 120, 105, 93, 79, 69, 55
β-Caryophyllene	10.361	204	204, 189, 175, 161, 147, 133, 120, 105, 93, 79, 69, 55
Limonene	7.214	136	136, 121, 93, 79, 68, 53

ond order (F2) kinetics. The experimental master plots were found to be significantly independent of heating rates confirming that $g(\alpha)$ varies with α without any effect of heating rate. The value of A was found to be 1.7×10^{10} min^{-1} (i.e., $ln\ A = 23.6$). The reconstructed plot from this data (Fig. 3b) closely resembled ($R^2 > 0.9$) the experimental plots upto α = 0.65, confirming the proposed mechanism. The average E_a value was found to be ~121 kJ mol^{-1}, which suggests relatively rapid volatilization of the material. The residue at 800 °C was analyzed by SEM-EDS and found to contain C, O, P, S, K, Mg, Ca, Al and Si to various extents; C and O were present in substantial amounts. This study shows that the incineration process does not completely destroy the drug, rather it throws large quantities of drug-related toxic substances into the environment.

3.1.1. Isothermal analysis

It was possible to construct isothermal time-α plots at different temperatures (Fig. 2f) from the data obtained from isoconversional analysis. The validity of the data was established by comparing an experimental plot at 473 K with that obtained from the calculated data; the two curves resembled very closely (Fig. 2f).

3.2. Pyrolysis GC–MS analysis

In order to find a suitable solvent for collecting the degradation products different solvents including acetone, methanol, *n*-hexane, carbon tetrachloride and chloroform were used. The *n*-hexane produced chromatogram showing separation of all the components reported in this work. Total ion chromatogram (TIC) along with

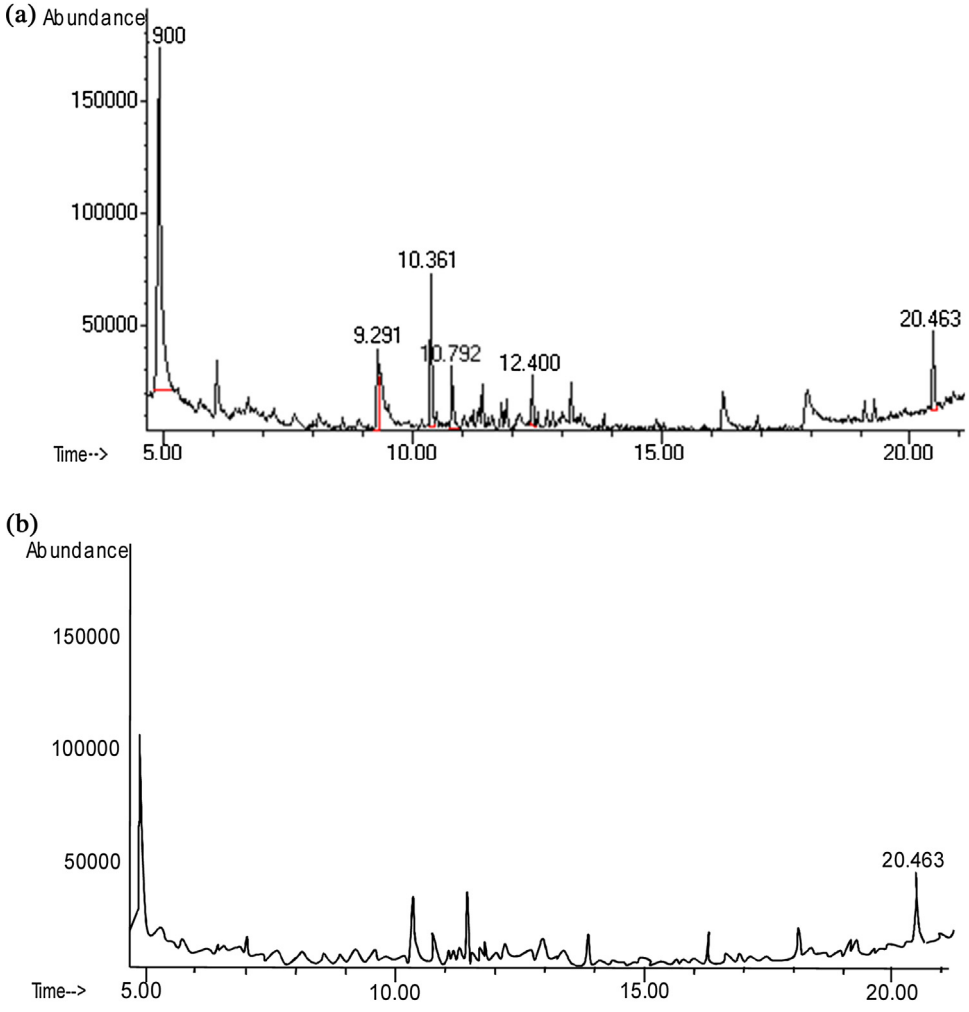

Fig. 3. Total ion chromatograms (a) hashih sample (b) signature compound.

the peak specific mass spectra obtained from *n*-hexane solution is shown in Fig. 3a.

In total fifteen numbers of peaks were recorded, out of which four could be correctly identified. The degradation products thus identified included: cannabidiol (CAS # 13956-29-1), limonene (CAS # 5989-27-5), α- (CAS # 6753-98-6) and β-caryophyllene (CAS # 87-44-5), mainly originating from the pyrolysis of hashish. These substances are known to have adverse effects on human health and cause an irreversible damage to the environment [14]. The other two products seemed to be the pyrolytic products of acetaminophen (CAS # 103-90-2) and *N*-[4-(vinyloxy)phenyl]acetamide (dehydrophenacetin, CAS # 830-04-6) which are the possible adulterants usually added to the market samples of hashish. Presumably these additives enhance the absorption of cannabinoids. The retention data and mass spectra relating to the major ions are listed in Table 2.

These results suggest that on destruction of ceased material by regulating agencies by way of incineration will throw a large quantity of particulate matter containing these toxic substances along with a part of sublimed disperse of ceased material.

3.2.1. Analysis of human tissue

All the three human lung tissue samples analyzed by the pyrolysis-GC–MS method showed the signature of cannabis as indicated by the characteristic peak due to cannabidiol (retention time = 20.463 min; Fig. 3b). Percent recovery, precision (RSD), limit of detection and limit of quantitation were found to be 85%, 0.35%, 1.5 ng mL^{-1} and 7.6 ng mL^{-1} respectively. This analysis suggests that the pyrolysis GC–MS method can be used to identify and quantify cannabinoids in biological samples. This method can be validated by further work.

3.3. Microscopic analysis of residue

The SEM images of the residues are shown in Fig. 4. The EDS profiling of the residue showed the presence of C, O, P, S, K, Mg, Ca, Al and Si elements in the samples as shown in Table 3. Among these elements the presence of Al is due to widespread use of aluminium foil used as a support for sublimation of hashish for direct inhalation and Si comes from soil contamination. The other elements are inherent to be contained in the resinous material.

4. Conclusions

Street samples of hashish were analyzed by isoconversional thermal and pyrolytic GC–MS analysis. The earlier water loss from the sample was followed by major decomposition in the temperature range 463–643 K. During this range some toxic substances produced have been identified by pyrolytic GC–MS analysis. These include cannabidiol, limonene, β-caryophyllene, acetaminophen

and dehydrophenacetin. The SEM-EDS analysis of the residue showed the presence of C, O, P, S, K, Mg, Ca, Al and Si elements. A multistep degradation mehcnaim has been suggested for thermal decomposition of hashish samples. Upon incineration of ceased material, several toxics are thrown into the environment that may cause its irreversible degradation and pose serious health hazards. The pyrolysis-GC–MS analysis also provides signatures of the drug in biological tissue.

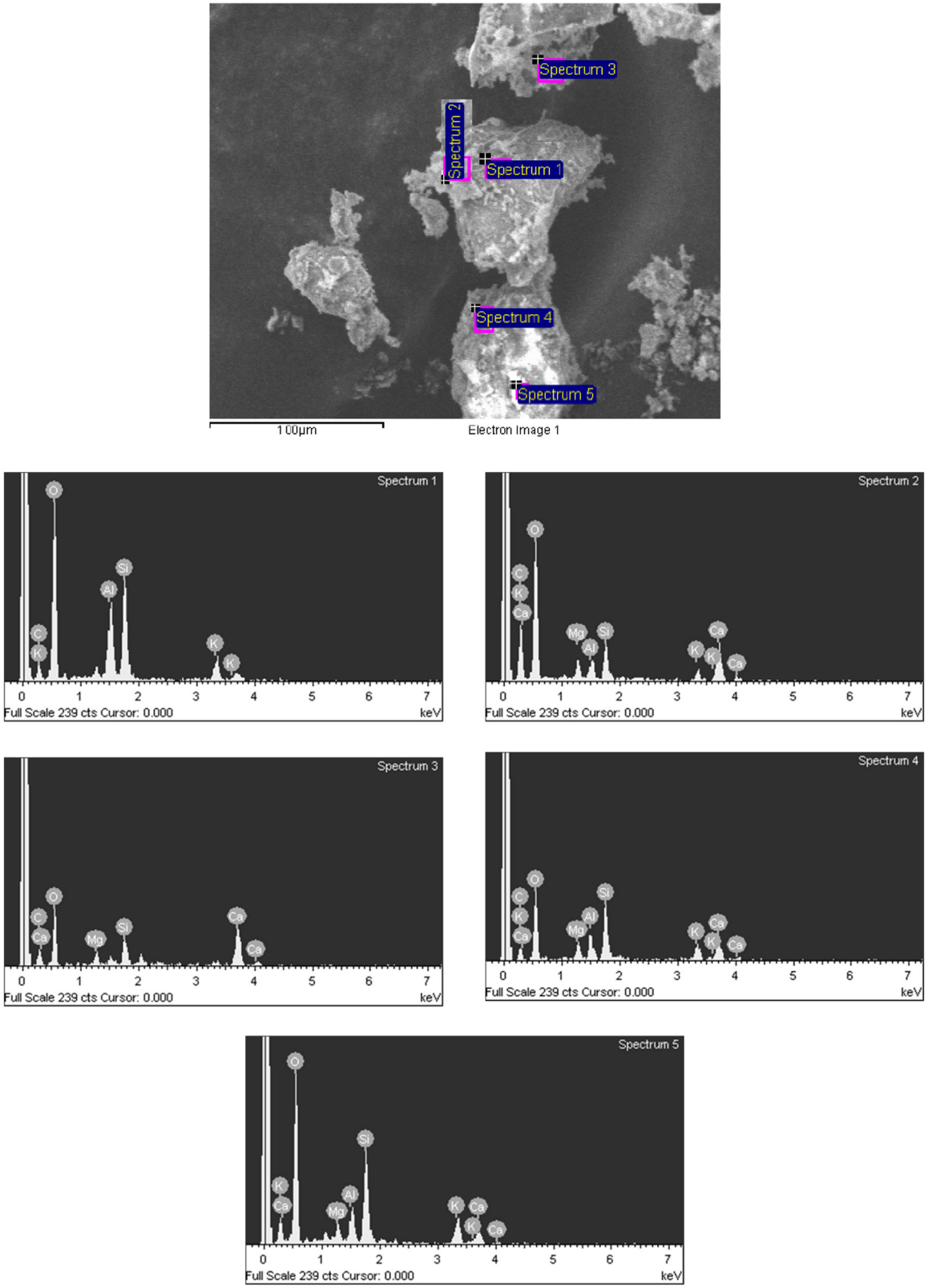

Fig. 4. SEM and EDS analysis of the residue from different points in the micrograph.

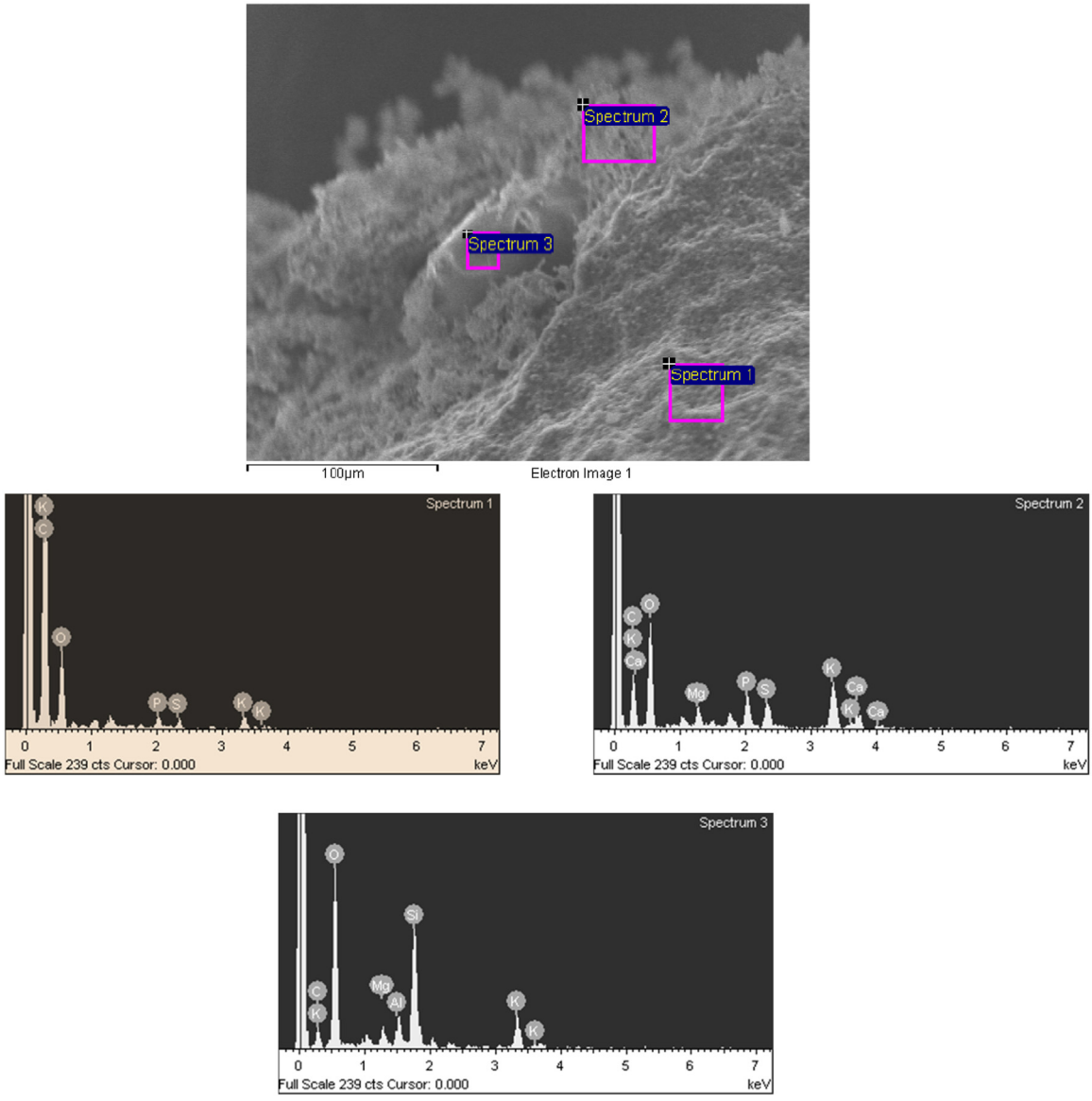

Fig. 4. (it Continued)

Table 3
EDS elemental analysis (%).

Element	Sample A					Sample B		
	Location					Location		
	1	2	3	4	5	1	2	3
C	4.49	24.4	19.84	11.64	–	65.32	23.15	11.36
O	69.82	61.84	60.36	60.73	72.77	32.65	58.23	66.49
P	–	–	–	–	–	0.58	3.78	2.91
S	–	–	–	–	–	0.5	3.04	12.45
Si	13.42	3.39	5.41	12.28	12.34	–	–	–
Mg	–	2.09	2.85	3.11	2.5	–	2.39	2
Al	8.31	1.74	–	3.16	4.6	–	–	–
K	3.95	1.28	–	4.1	4.95	0.95	6.87	4.79
Ca	–	5.27	11.54	4.98	2.84	–	2.55	–

References

[1] M.A. ElSohly, D. Slade, Chemical constituents of marijuana: the complex mixture of natural cannabinoids, Life Sci. 78 (2005) 539–548.
[2] A.W. Zuardi, History of cannabis as a medicine: a review, Rev. Bras. Psiquiatr. 28 (2006) 153–157.
[3] M.G. Klous, G.M. Bronner, B. Nuijen, J.M. van Ree, J.H. Beijnen, Pharmaceutical heroin for inhalation: thermal analysis and recovery experiments aftere volatilisation, J. Pharm. Biomed. Anal. 39 (2005) 944–950.
[4] M.J. Starink, The determination of activation energy from linear heating rate experiments: a comparison of the accuracy of isoconversion methods, Thermochim. Acta 404 (2003) 163–176.

[5] J. Akbar, M.S. Iqbal, S. Massey, R. Masih, Kinetics and mechanism of thermal degradation of pentose- and hexose-based carbohydrate polymers, Carbohydr. Polym. 90 (2012) 1386–1393.
[6] M.S. Iqbal, J. Akbar, S. Saghir, A. Karim, A. Koschella, T. Heinze, Thermal studies of plant carbohydrate polymer hydrogels, Carbohydr. Polym. 86 (2011) 1775–1783.
[7] S.C. Turmanova, S.D. Genieva, A.S. Dimitrova, L.T. Vlaev, Non-isothermal degradation kinetics of filled with rise husk ash polypropene composites, Express Polym. Lett. 2 (2008) 133–146.
[8] B. Janković, Kinetic analysis of the nonisothermal decomposition of potassium metabisulfite using the model-fitting and isoconversional (model-free) methods, Chem. Eng. J. 139 (2008) 128–135.
[9] S. Vyazovkin, A.K. Burnham, J.M. Criado, L.A. Pérez-Maqueda, C. Popescu, N. Sbirrazzuoli, ICTAC Kinetics Committee recommendations for performing kinetic computations on thermal analysis data, Thermochim. Acta 520 (2011) 1–19.
[10] R. Lewis, S. Ward, R. Johnson, D.T. Burns, Distribution of the principal cannabinoids within bars of compressed cannabis resin, Anal. Chim. Acta 538 (2005) 399–405.
[11] J.H. Liu, M.P. Fitzgerald, G.V. Smith, Mass spectrometric characterization of cannabinoids in raw Cannabis sativa L. samples, Anal. Chem. 51 (1979) 1875–1877.
[12] H.B. Sowbhagya, P. Srinivas, N. Krishnamurthy, Effect of enzymes on extraction of volatiles from celery seeds, Food Chem. 120 (2010) 230–234.
[13] T.B. Vree, Mass spectrometry of cannabinoids, J. Pharm. Sci. 66 (1977) 1444–1450.
[14] S. Agurell, The Cannabinoids: Chemical, Pharmacologic, and Therapeutic Aspects, Academic Press, 1984.